06

Effect of accelerated high-energy electrons with low absorbed doses on the structure of polyimide press material

© V.I. Pavlenko,[1] N.I. Cherkashina,[1] A.V. Noskov,[2] O.D. Edamenko,[1] Z.V. Pavlenko,[1] S.V. Serebryakov[1]

[1] Belgorod State Technology University named after V.G. Shukhov,
308012 Belgorod, Russia
[2] Moscow Technical University of Communications and Informatics (MTUCI),
111024 Moscow, Russia
e-mail: Serebr43@yandex.ru

Received July 15, 2024
Revised November 14, 2024
Accepted November 18, 2024

The influence of high energy accelerated electrons ($E = 5$ MeV) and low absorbed doses ($D = 5-50$ kGy) on structural and X-ray dislocation parameters of amorphous-crystalline polyimide press-material PI-PR-20 has been investigated by XRD method. Destruction of polyimide macromolecules at absorbed doses of 5−25 kGy is accompanied by destruction and additional amorphization of macromolecules (domains). At $D = 50$ kGy, polymerization and crystallization of macromolecules occur with the formation of crystallites with denser packing, increased size of the coherent scattering area and minimal microdistortion of the crystalline lattice of crystallites.

Keywords: polyimide, X-ray phase analysis, X-ray structural analysis, amorphous halo, polymer domains and crystallites, coherent scattering region (CSR), dislocation parameters, microdistortions.

DOI: 10.61011/TP.2025.04.61212.235-24

Introduction

In order to create modern composite aerospace materials, polycondensational polymers based on polyimide binders are widely used [1–3].

Polyimides contain articulated atoms in a diamine fragment of the molecule, thereby providing high elastic and deformational properties of the polymer. The polyimide of the PI-PR-20 grade has the following structure [4–6]:

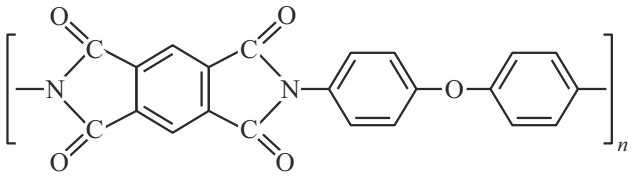

(1)

The aromatic polyimides (PI) are promising materials for producing protective coating of structural elements of spacecrafts [7–11]. The polyimides have a number of unique properties: thermal stability (up to 500 °C), cryogenic resistance (up to −200 °C), radiation resistance (100−200 MGy), mechanical tensile strength (up to 100 MPa), fire resistance, high resistances to proton and electron radiation, fluxes of charged heavy ions and to deep vacuum [3,12–13]. In this regard, it is necessary to specify critical parameters of impact of negative space factors on stability of physical & technical PI properties and the composites based thereon.

The biggest attention of the researchers in the field of polymer space material science is paid to the polyimide films of the type PM-1E and Kapton-100 HN.

One of the promising polymer matrices for creation of the structural composite based thereon is a thermoplastic press-powder of the grade PI-PR-20, which has amorphous-crystalline structure. The polyimide polymers have a chain structure [4–6].Presence of conformation disordering of the polymer macromolecules and steric difficulties due to an amorphous phase create certain obstacles for correct packaging of the PI macromolecules during chemical crystallization in a melt in the presence of special initiators at the high temperatures. (320−350 °C) [4,14].

Importance of PI crystallization lies in improved thermal and thermal-oxidative stability, higher physical & mechanical and adhesion characteristics as well as the capability of melt retreatment, i.e. the capability of keeping a crystallite state after polymer melting [4,14].

In order to solve this problem, scientific and practical interest is paid to directional solidification of PI under impact of electron irradiation of the polymer. The work [15] has studied impact of electron interaction with low-energy ($E = 0.5$ MeV) high absorbed doses ($D = 1-300$ MGy) on the PI films in order to investigate the radiation resistance

Motion of the accelerated electrons in a material is accompanied by their deceleration. The electrons lose their energy as a result of inelastic collision with atoms and molecules of the material. The energy of the electron beam is transferred as a result of collisions with the polymer target. As a result of fast heating under electron irradiation, the process is quasi-adiabatic [9,15–20].

When the accelerated electrons collide with the PI, complex competing processes are undergoing: ruptures of macrochains (destructions) intermolecular stitching (structuring) of activated macromolecules [12,13,21].

The present work studies impact of high-energy ($E = 5$ MeV) accelerated electrons with the low absorbed doses ($D = 5-50$ kGy) on the capability of crystallization of the polyimide of the PI-PR-20 grade. It uses X-ray diffraction method of analysis.

1. Materials and research methods

1.1. Preparation of samples

The research object was thermoplastic polyimide press-powder PI-PR-20 (TU 6-06-239-92). The size of the particles is $5-8\,\mu$m, and the density is 1.42 g/cm^3. The PI press-powder was pressed under the specific pressure of 120 MPa and at the room temperature into cylindrical tablets of the diameter of 4.0 cm, and the height of 0.6 cm. The density of the pressed PI is 1.76 g/cm^3.

1.2. Irradiation of samples by accelerated electrons

The PI samples were irradiated on the linear VHF electron accelerator „Raduga" in FSPC „RAS MRTI". The electron energy was 5 MeV, the electron beam power was 1.5 kW, the electron fluence was $3 \cdot 10^{16}$ electron/(cm$^2 \cdot$ s), the size of the effective area of the electron beam was 50×50 mm. The irradiation by the accelerated electrons was in air. During irradiation, the maximum temperature of the polymer samples was 50 °C.

1.3. Research methods

1.3.1. X-ray phase analysis and X-ray diffraction analysis

The X-ray diffraction analysis (XDA) was performed on the X-ray diffractometer DRON-3 with the CuK_α-anode ($\lambda = 1.5406$ Å) and the Ni-filter by the powder method (of the Debye–Scherrer polycrystal). The spectrum was recorded by an ionization meter MSTR-4 within the range of the angles 2θ from 4 to 64° (the step 0.050, the accumulation time 10 s). Using the PowderCell software, parameters of the X-ray characteristics of the spectrum were defined.

1.3.2. X-ray dislocation parameters

The sizes of the coherent scattering region (CSR) and microdistortions of crystallites in PI were calculated as per the Selyakov–Scherrer method [22,23] by FWHM of the diffraction reflection. Using the PowderCell software, the following parameters of the diffraction pattern were determined: the Bragg angle 2θ, the peak width (β) at the FWHM, microdistortion ($\Delta d/d$) of the PI crystallites.

The CSR size, D, [Å]:

$$D = \frac{0.97\lambda_{\mathrm{CuK}\alpha}}{\beta \cos\theta}, \tag{2}$$

where $\lambda_{\mathrm{CuK}\alpha}$ — the wavelength of used radiation, [Å]; θ — the angular position of maximum (the diffraction angle), [deg]; β — FWHM, [rad].

Microdistortion of the crystal $\Delta d/d$:

$$\frac{\Delta d}{d} = \left(\frac{\beta \mathrm{rad}}{4\,\mathrm{tg}\,\theta}\right). \tag{3}$$

2. Discussion of the results

2.1. Modeling of passing of accelerated electrons

The spatial distribution of primary and secondary electrons was modeled by using an atomic composition of the polymer, which is defined by energy-dispersive X-ray spectroscopy (EDS): mass%: C — 82.0; O — 13.3; N — 4.7 and its density in the pressed form, which is 1.76 g/cm^3.

Scattering of fast electrons inside the PI has been calculated as per the Rao–Sakhiba–Vitri model which is a modification of the classic theory of scattering of charged particles in the substance (the Bethe–Bloch model) [17,18]. Spatial distribution of the primary and secondary electrons with energy through the PI is modeled as per the Monte–Carlo method [18] in the considered energy range (0.5–5.0 MeV) when the electron falls at a right angle to the surface of the cylindrical polymer.

The electrons moving in a solid body primarily experience ionization and radiation losses.

Fig. 1 shows calculations of the dependence of specific ionization and radiation losses of accelerated electron in PI on the kinetic energy of the electron within the energy range (0.5–5.0 MeV). It is clear from Fig. 1 that the main process of energy transfer to PI is ionization losses. For the energy of the accelerated electrons of 5 MeV, the specific ionization $(-dE/dx)_{col}$ and radiation $(-dE/dx)_{rad}$ energy losses in the PI material are 5.91 and 0.15 MeV/cm, respectively, i.e. the specific ionization losses in PI exceed the specific radiation losses approximately in 40 times.

Fig. 2 shows comparative curves of the specific ionization and radiation losses on the same graph as well as a curve describing the total losses (0.5–5.0 MeV) of the electron energy.

The total electron energy losses in PI are determined as follows:

$$\left(-\frac{dE}{dx}\right) = \left(-\frac{dE}{dx}\right)_{col} + \left(-\frac{dE}{dx}\right)_{rad}, \tag{4}$$

where dE — the energy lost by the particle in the substance layer of the thickness of dx; $(-dE/dx)_{col}$ — specific ionization losses; $(-dE/dx)_{rad}$ — specific radiation losses.

Since the electron energy losses in the materials results in its deceleration, then it is possible to determine an average range of the electron during its deceleration provided that the electron continuously losses the energy along the entire path in accordance with decelerability $(-dE/dx)$. The true

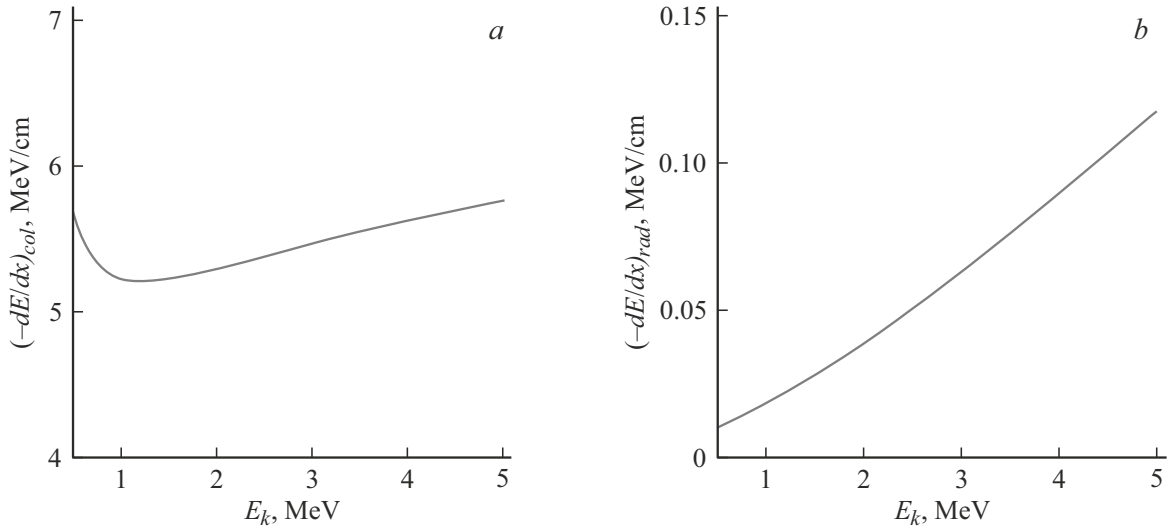

Figure 1. Dependence of specific ionization (a) and radiation (b) losses of accelerated electrons in PI on its initial kinetic energy.

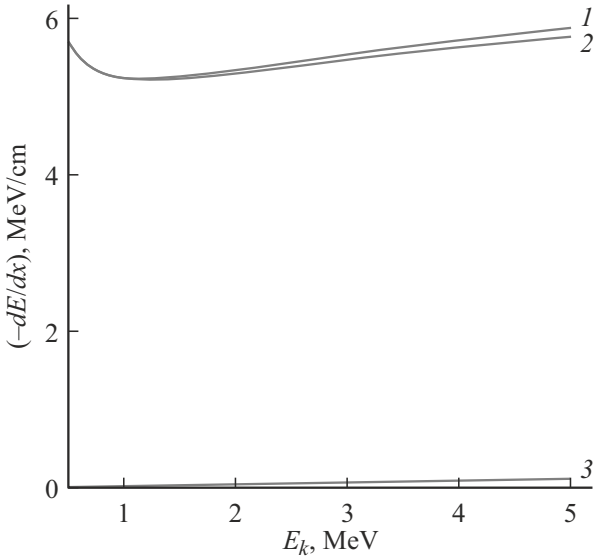

Figure 2. Dependences of the specific full energy losses of the accelerated electron in PI on its kinetic energy: *1* — the total losses (0.5–5.0 MeV) the electron energy; *2* — ionization losses; *3* — radiation losses.

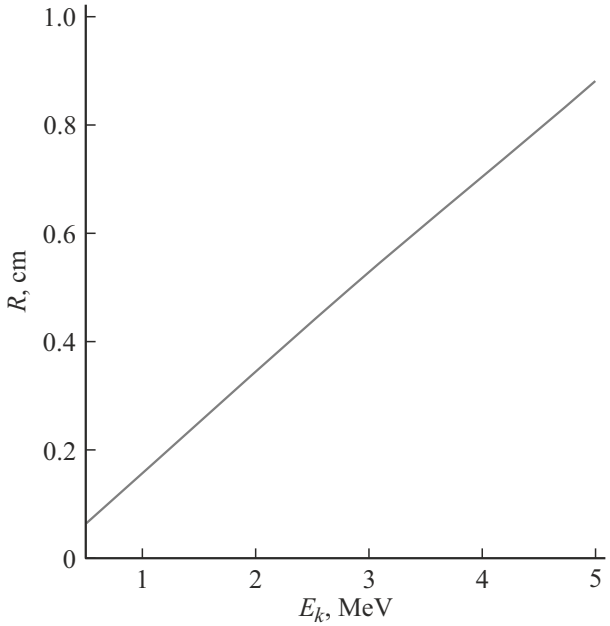

Figure 3. Dependence of the average range of the electron in PI on its initial kinetic energy.

ranges are random and distributed around an average range which is calculated by the formula [5]:

$$R(E_0) = \int_0^{E_0} \frac{dE_k}{(-dE/dx)}, \tag{5}$$

where E_0 — the initial electron energy; dE_k — the energy lost when passing through the material.

Fig. 3 shows the graph which demonstrates the dependence of the average range of the accelerated electron in PI on its initial kinetic energy. For the examined polymer target the average electron range with the energy of 5 MeV is about 0.83 cm. One of the main factor to provide homogeneity of PI irradiation by accelerated electrons is typical distribution of energy and absorbed dose of electron irradiation along the polymer depth.

The energy transmission coefficient $T_E(x)$ is equal to a ratio of the energy of all the particles passed over the path $E(x)$ in PI to the energy of all the fallen particles:

$$T_e(x) = \frac{E(x)}{N_0 E_0}, \tag{6}$$

where N_0 — the number of electrons fallen to the target.

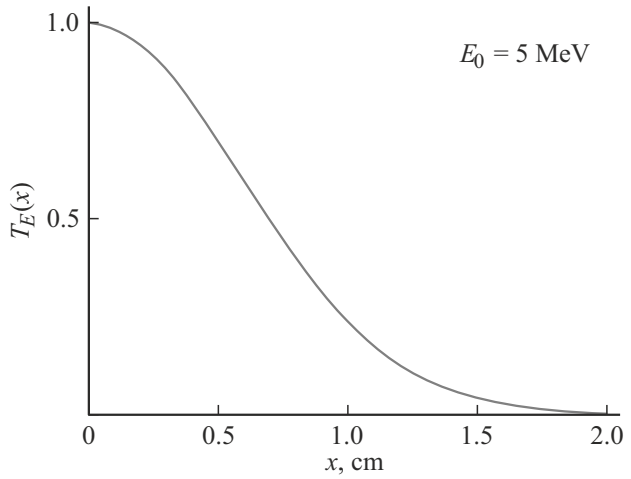

Figure 4. Dependence of the energy transmission coefficient of the accelerated electron on the depth (x) of PI.

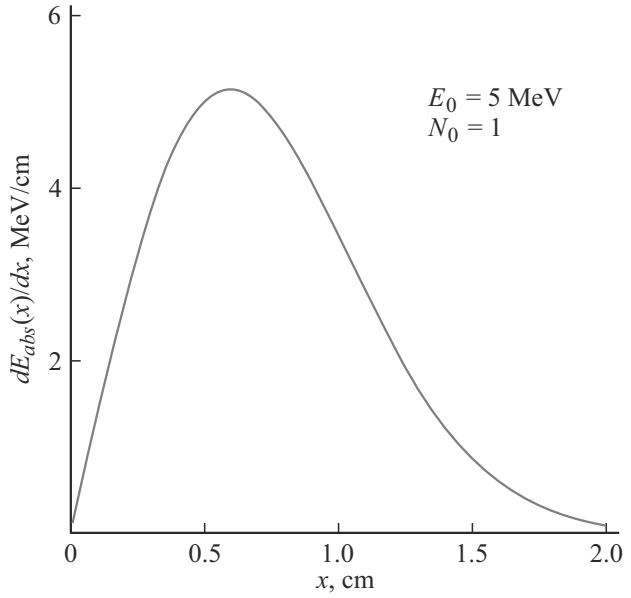

Figure 5. Distribution of the absorbed energy of the accelerated electron along the depth (x) of PI.

Based on the Monte–Carlo method, passage of the electron through PI was numerically modeled to obtain the function $T_E(x)$, which is plotted in Fig. 4. The curve shows the dependence of the absorbed electron energy along the PI depth. At the same time, the maximum of distribution of the absorbed energy of electron irradiation in PI is at the depth $x \approx 0.6$ cm (Fig. 5).

In accordance with [24], such form of distribution of absorbed energy along the depth of the solid body is mainly due to repeated scattering of the primary electrons and generation of the secondary electrons. When the electrons are decelerated in a medium, the ionization losses increase and the number of the secondary electrons grows. As a result, the medium atoms ionization density increases, so does therefore the energy absorbed in the substance. On the other hand, repeated scattering of the primary electrons result in scattering of their ranges, thereby reducing the number of electrons moving in the initial direction of the beam and the number of back-scattered electrons. Presence of these two processes with the big number of electrons in the beam results in generation of a wide superposition maximum in distribution of energy along the material depth.

It is necessary to note that distribution of the absorbed dose (5, 25 and 50 kGy) of electron irradiation along the polymer depth will be of the same form.

2.2. X-ray diffraction studies

The diffraction pattern of X-ray radiation scattering of the initial PI means presence of the amorphous and the crystallite phases which is manifested in the XDA X-ray diagram of the amorphous halo within the range $2\theta = 20-30^\circ$ and superposition of the discrete reflections within the range $2\theta = 4-64^\circ$.

It is known that the density of the polymer material of the amorphous phase slightly differs from the crystal density. According to [3], for the polymers the molecule packaging coefficients in the crystallite (K_{cr}) state and the amorphous state (K_{am}) are almost constant, while the ratio $K_{cr}/K_{am} = 1.1$.

The amorphous halo of the initial PI within the range $2\theta = 20-30^\circ$ is determined by two typical interplanar spacings: interchain and along-chain macromolecules of the approximately same intensity in the middle range with $d = 3.948$ and 3.312 Å, thereby meaning the close packing of the macromolecules in PI (Fig. 6, *d*). The widened amorphous halos contain discrete reflections that correspond to the PI crystallite phases.

With electron irradiation of PI with the minimum absorbed dose ($D = 5$ kGy) there was observed superposition of the two amorphous halos into a widened one with increase of its relative intensity ($\sim$ in two times). The average interplanar spacing increased to $d = 4.506$ Å to generate a less ordered structure of the short-range order (domain).

A general type of the amorphous halo of electron-irradiated PI with the absorbed dose of 25 kGy has not changed (Fig. 6). Additional widening of the amorphous halo (up to $\Delta = 21^\circ$), in accordance with the Selyakov–Sherrer equation [25], indicates reduced sizes of the generated oligomer amorphous PI macromolecules. It can be caused by destruction of the PI macromolecules.

It can be supposed that there is probability of free-radical reactions in PI by electron irradiation already at the low absorbed doses ($D = 5-25$ kGy) in a high-energy flux of accelerated electrons ($E = 5$ MeV), disruption of the microstructure of imide chains of the polymer and defect formation in the imide cycles.

The amorphous halo of the X-ray diffraction pattern is asymmetrical. The asymmetry of the isotropic macro-

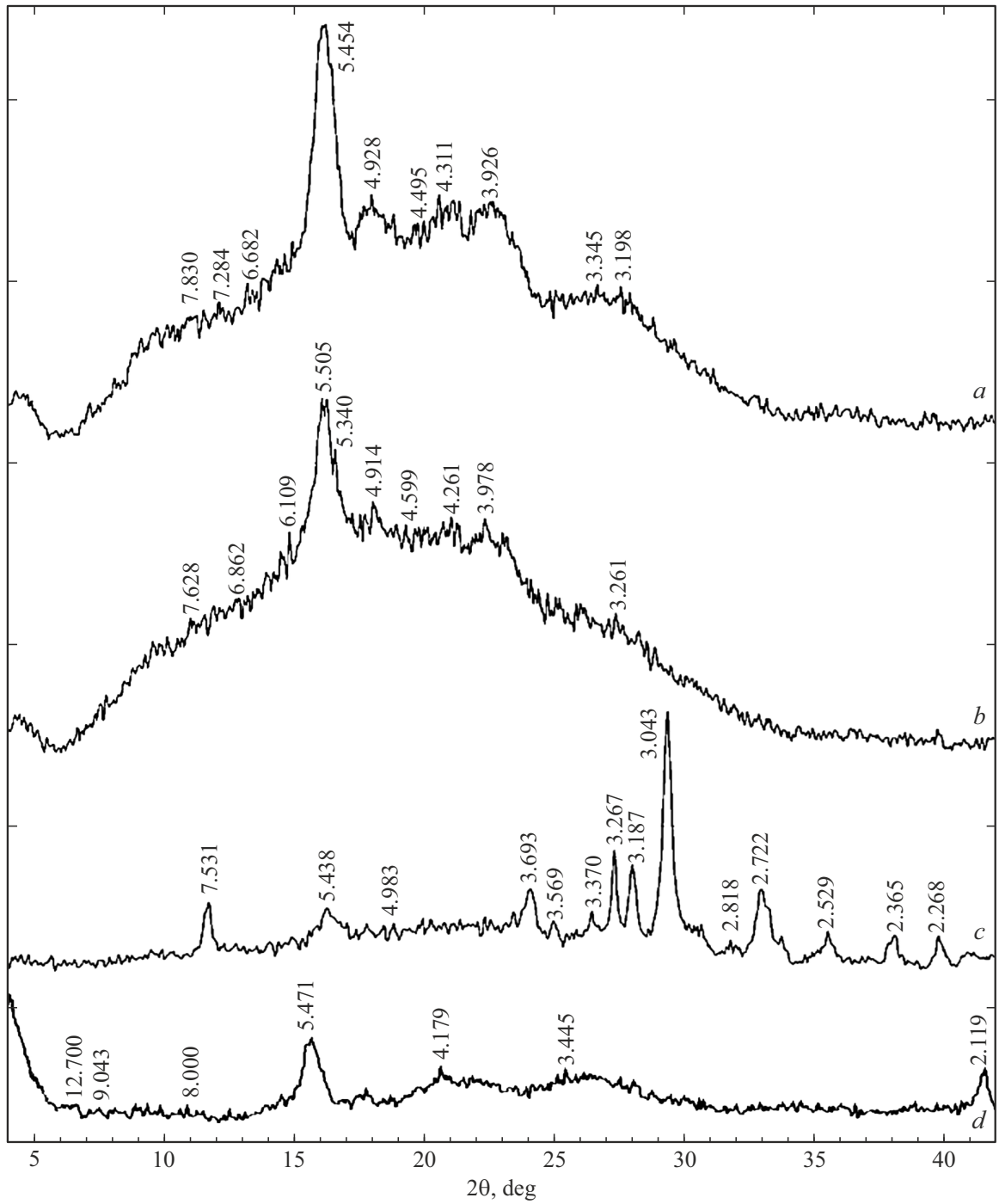

Figure 6. Diffraction pattern of PI-PR-20 before irradiation and the one irradiated by the accelerated electrons ($E = 5$ MeV) with various absorbed doses: *a* — 5, *b* — 25, *c* — 50 kGy; *d* — unirradiated.

molecules is a common property of the polymers with a spiral structure and a chain structure, which characterized the presence of the short-range order constant [26]. The presence of quite intensive diffraction reflections within the Bragg angles for the amorphous halo ($2\theta = 20-30^\circ$) is typical for the anisotropic crystallites distributed in the structure of the amorphous matrix, thereby indicating the presence of a long-range order in PI.

In accordance with [27], the most probable permolecular PI structures is considered to be a lattice, where dianhydride and diimine fragments of various molecules are located in alternating layers.

When increasing the absorbed dose to 50 kGy, the intensity of the amorphous halo on the X-ray diffraction pattern of XPA (Fig. 6) is sharply reduced, thereby indicating an intense process of crystallization in PI.

The sharp reduction of intensity of the amorphous halo with the absorbed dose of 50 kGy can result from radiation stitching of the activated oligomer macromolecule with generation of the crystallites during the crystallization. In accordance with [27–30], the stitching mechanisms of PI macromolecules can undergo via reactions between neighboring imide cycles with generation of intermolecular bonds.

The XPA diffraction pattern of the initial PI exhibits two quite intensive and clear reflections at $2\theta = 5.20$ and 16.20°, which, as per [27], are a result of reflection from the planes ($hkl = 002$) and (110), thereby resulting in generation of ordered short-range order regions (domains) with $d = 14.799$ and 5.471 Å respectively (Fig. 6).

The diffraction reflections at $2\theta = 5.2$ and 16.2° are of a widened type: FWHM is $\Delta = 2.6$ and 1.39° , respectively, thereby indicating disruption of the microstructure in the crystallite PI phases.

The XPA diffraction pattern has the most intensive reflections recorded (d): 5.471 Å ($I = 100\,\%$); 3.404 Å (61.2 %); 4.160 Å (59.7 %); 3.312 Å (58.7 %); 3.239 Å (57.8 %); 3.353 Å (54.5 %); 3.445 Å (53.5 %); 3.965 Å (53.0 %); 3.840 Å (50.3 %); 3.151 Å (50.2 %); 3.534 Å (47.5 %); 53.811 Å (46.3 %); 3.705 Å (44.3 %); 3.678 Å (42.5 %); 3.610 Å (36.7 %).

Thus, it can be stated that the crystallite phase in the initial polyimide polymer has ordering with defectiveness of the crystallite lattice.

Electron irradiation of PI with the absorbed dose of 5 kGy had resulted in the fact that the most defective crystallites at $2\theta = 5.2°$ with a high value of the interplanar spacing ($d = 14.799$ Å) were not revealed on the XPA diffraction pattern, while the relative intensity of the reflection at $2\theta = 16.2°$ ($d = 5.471$ Å) noticeably increased ($\sim$ in two times) with mixing to $d = 5.488$ Å and reduction of its half width from $\Delta = 1.39°$ (the initial polymer) to $\Delta = 0.82°$ (Fig. 6, *a*). Thus, the electron irradiation of PI with the absorbed dose of 5 kGy resulted in increase of ordering of these crystallites in a certain degree with preferable orientation in the plane (110).

The general type of the XPA diffraction pattern of the polymer irradiated by electrons within the doses $D = 5-25$ kGy was not changed. However, a denser crystallite structure was being formed; the interplanar spacing distance in the polymer matrix was being reduced from $d = 5.488$ Å ($D = 5$ kGy) to $d = 5.464$ Å ($D = 25$ kGy). The half width of reflection at $d = 5.464$ Å increased from $\Delta = 0.82°$ ($D = 5$ kGy) to $\Delta = 1.02°$ with simultaneous reduction of its relative intensity. Therefore, within the absorbed doses $D = 5-25$ kGy of radiation irradiation of the polymer there was formation of highly-defective crystallites with the denser structure.

With increase of the absorbed dose of the accelerated electrons to 50 kGy, there were the most significant structure & phase transformations observed in PI. The relative intensity of the crystallite reflection on the X-ray XPA diffraction pattern (Fig. 6, *c*) at $2\theta = 16.1°$ ($d = 5.464$ Å; $I = 100\,\%$) was sharply reduced with increase in defect formation ($\Delta = 1.28°$) in the crystallites of this phase. At the same time, there was registered formation of a new crystallite phase at $2\theta = 29.3°$ ($d = 3.043$ Å; $I = 100\,\%$), which is indicated by intensive and quite narrow ($\Delta = 0.58°$) reflection. We can assume that there is a process of recrystallization of crystallites, which were observed within the absorbed doses (0–25 kGy) and transformation into a new crystallite phase with a more close packing of the polymer molecules at the increased absorbed dose ($D = 50$ kGy) of the accelerated electrons ($E = 5$ MeV).

We also register the other most intensive diffraction reflections of the new crystallite phase, which were formed at $D = 50$ kGy of the accelerated electrons ($E = 5$ MeV): $d = 3.043$ Å ($I = 100\,\%$); 3.267 Å (42.8 %); 3.187 Å (40.1 %); 3.700 Å (32.3 %); 2.718 Å (32.2 %); 7.563 Å (24.8 %); 5.454 Å (24.1 %); 3.376 Å (21.0 %); 4.385 Å (18.4 %); 4.461 Å (18.1 %); 4.281 Å (17.9 %).

Thus, distinct change of the peak intensity at $2\theta = 5.4-5.50°$, which exhibits at sharp increase at the irradiation dose 5–25 kGy, is explained by radiation destruction of the PI macromolecules with generation of oligomer amorphous macromolecules, defect formation in the crystal phase of the polymer and collapse of the polycrystals that later disintegrate into smaller segments and become denser (which is indicated by small decrease of the FWHM at 25 kGy, in relation to 5 kGy). However, increase of the absorbed dose increases the number of defects, thereby reducing the peak intensity. This results in recrystallization of the crystallites, which further, with at the absorbed dose of 50 kGy, is exhibited by sharp reduction of intensity of the peak $2\theta = 5.4-5.50°$ and formation of the new crystallite phase at $2\theta = 29.30°$ with a closer packing of the polymer macromolecules. These changes are explained by radiation stitching of the activated oligomer macromolecule with generation of the crystallites during crystallization due to a reaction between the adjacent imide cycles and with generation of the intermolecular bonds, which can result from appearance of reactive oxygen and nitrogen in the polyimide structure during destruction of the crystals. After that oxygen and nitrogen result in appearance of other compounds due to newly-generated bonds CH_2-O and C≡N [27].

2.3. Dislocation structures of PI

The main parameters of the crystallite phase include the width of the diffraction peaks, the CSR sizes and microdistortions ($\Delta d/d$) of the crystals. The CSR sizes in the crystallite phases of PI are determined by widening of the diffraction reflections and used for evaluating the crystallite sizes (see Table).

The change of the X-ray PI parameters during irradiation by the accelerated electrons within the absorbed doses ($D = 5-50$ kGy) resulted in the change of the dislocation parameters of the polymer crystallite phases.

X-ray dislocation parameters of PI irradiated by electrons ($E = 5$ MeV)

Parameter	Absorbed dose, kGy			
	0	5	25	50
Bragg diffraction angle, 2θ	16.2	16.1	16.3	29.3
Interplanar spacing, d (Å)	5.471	5.488	5.464	3.043
Diffraction peak width, β	0.93	1.40	1.10	0.58
Peak width (β_{rad}) at half maximum FWHM, rad	0.0162	0.0244	0.0192	0.0101
CSR size (D), Å (OCSR for the reference (Ceylon graphite ~ 1200 Å [31])	93	62	79	153
Microdistortion of crystal $\Delta d/d$, rel.un.	$2.9 \cdot 10^{-2}$	$4.3 \cdot 10^{-2}$	$3.3 \cdot 10^{-2}$	$9.4 \cdot 10^{-3}$

There was observed increase of the CSR size in transition from 93 Å for the crystallites with $d = 5.471$ Å ($I = 100\,\%$) in the initial polymer 153 Å after electron irradiation ($D = 50$ kGy) for the crystallites with $d = 3.043$ Å ($I = 100\,\%$). Intensive PI amorphization under electron irradiation with $D = 5-25$ kGy resulted in reduction of the CSR sizes (see Table).

Increase of the CSR sizes for the crystallites in PI irradiated at $D = 50$ kGy was accompanied by noticeable reduction ($\sim$ in 3.5 times) of the magnitude of crystallite microdistortion (see Table). The positive values of the microdistortion magnitudes ($\Delta d/d$) within the absorbed doses ($D = 0-50$ kGy) of electron irradiation of PI indicated tensile strain in the crystallite phases as a result of plastic strain of the polymer macromolecules.

During irradiation of the polyimide by electrons, it is possible that the values of contact angle of wetting by water are reduced due to increase of roughness of the material surface. Darkening of the polyimide is also possible, thereby resulting in fall of light transmission values. Besides, it is known about increase of tensile strength, percent elongation, i.e. the change of the material length to its initial length after load, and strain energy [30]. The dose of 23 kGy reduces the polyimide melting temperature from 387 °C to 380 °C. Electron irradiation may include output of gases from the polyimide volume, such as H−OH, NH, oxygen, thereby resulting in reduction of free volume inside the material, and it can also explain a process in which the material roughness is increased. Irradiation by electrons with the energy of 1 MeV and higher results in decrease of dielectric permittivity [32].

Conclusion

Impact of the high-energy ($E = 5$ MeV) accelerated electrons with a relatively low absorbed dose ($D = 5-50$ kGy) on the amorphous-crystalline polyimide press-powder PI-PR-20 resulted in a process of complex structure & phase transformations. With the absorbed dose 5−25 kGy, there was radiation destruction of the PI macromolecules with generation of the oligomer amorphous macromolecules and defect formation in the crystalline phase of the polymer. The increase of the absorbed dose of electron irradiation to 50 kGy resulted in stitching of the radiation-activated macromolecules, recrystallization of the crystallite into the new crystallite phase ($d = 3.043$ Å) with closer packing of the macromolecules, reduced defectiveness of the crystallites and the increase of the CSR sizes.

Funding

The study was performed under the state assignment of the Ministry of Education and Science of the Russian Federation №FZWN-2023-0004. The equipment provided by the High-Technology Center of the Belgorod State Technology University named after V.G. Shukhov was used experiments.

Conflict of interest

The authors declare that they have no conflict of interest.

References

[1] S.V. Kryuchkova, M.Yu. Yablokova, A.Yu. Alentiev, L.G. Gasanova, A.V. Kepman. Vestnik MGU, ser. 2, Khimiya, **58** (3), 126 (2017). (in Russian)

[2] H. Ohya, V.V. Kudryavtaev, S.I. Semenova. *Polyimide Membranes: Applications, Fabrications, and Properties* (CRC Press, London, 1997), p. 314. https://doi.org/10.1201/9780203742969

[3] M.I. Bessonov, M.M. Koton, V.V. Kudryavtseva, L.A. Laius, *Poliimidy — klass termostoikikh polimerov* (Nauka, M., 1983), s. 328. (in Russian)

[4] U.S. Andropova, O.A. Serenko, E.S. Afanas'ev, D.A. Sapozhnikov, V.N. Chernik, L.S. Novikov. Poverkhnost, rentgenovskie, sinkhrotronnye i neitronnye issledovaniya, **8**, 3 (2022). (in Russian) DOI: 10.31857/S1028096022080027

[5] V.M. Svetlichnyi, V.V. Kudryavtsev. Vysokomolek. soed. seriya B, (in Russian) **45** (6), 984 (2003).

[6] T.H. Hou, J.M. Bai, T.L. St. Clair. *Polyimides: Materials, Chemistry and Characterization,* ed. by C. Feger, M.M. Khojasteh, J.E. McGrath (Elsevier, Amsterdam, 1989), p. 169.

[7] O.A. Anan'eva, V.K. Milinchuk, D.L. Zagorskii. Khimiya vysokikh energiy, **41** (4), 271 (2007). (in Russian)
[8] V.K. Milinchuk, E.R. Klinshpont, I.P. Shelukhov. Izvestiya vuzov, ser. yadernaya energetika, **2**, 108 (2002). (in Russian)
[9] O.F. Pasevich. *Issledovanie svoistv i struktury poliimidnykh plenok posle vozdeistviya faktorov kosmicheskogo prostranstva nizkikh zemnykh orbit* (Kand. diss. NIFKhI im. L.Ya. Karpova, M., 2006), 22 s. (in Russian)
[10] D.J. Liaw, K.L. Wang, Y.C. Huang, K.R. Lee, J.Y. Lai. C.S. Ha. Prog. Pol. Sci., **37**, 907 (2012). https://doi.org/10.1016/j.progpolymsci.2012.02.005
[11] I. Gouzman, E. Grossman, R. Verker, N. Atar, A. Bolker, N. Eliaz. Appl. Adv. Mater., **31** (18), 1807738 (2019). https: //doi.org/10.1002/adma.201807738
[12] V.K. Milinchuk, V.I. Tupikov. *Radiatsionnaya stoikost' organicheskikh materialov* (Energoatomizdat, M., 1986), 271 s. (in Russian)
[13] V.N. Kuleznev, *Chimiya i fizika polimerov* (Khimiya, M., 1988), 312 s. (in Russian)
[14] Yu.V. Shutilin. *Fiziko — khimiya polimerov* (PoliMir, Voronezh, 2012), 838 s. (in Russian)
[15] N.I. Cherkashina, V.I. Pavlenko, V.M. Abrosimov, V.I. Trofimov, S.V. Budnik, R.S. Churyukin, V.M. Gavrish. Acta Astronautica, **184**, 59 (2021). DOI: 10.1016/j.actaastro.2021.03.032
[16] E.N. Kablov, O.V. Startsev, I.G. Deev, E.F. Nikishin. Vse materialy. Entsiklopedicheskii spravochnik, **10**, 40 (2012). (in Russian)
[17] A.I. Akishin. *Razvitie kosmicheskogo materialovedeniya v NIIYaF MGU. 50 let NII yadernoi fiziki* (MGU, M., 1997), 87–234. (in Russian)
[18] M. Kotera. J. Appl. Phys., **52**, 997 (1981).
[19] A.I. Akishin, V.B. Baikal'tsev, Yu.I. Tyutrin. *Vozdeistvie elektronnykh potokov na zashchitnye pokrytiya solnechnykh batarei* (Atomizdat, M.,1991), 69 s. (in Russian)
[20] V.I. Pavlenko, N.I. Cherkashina, A.V. Noskov. Poverkhnost'. Rentgenovskie, sinkhrotronnye i neytronnye issledovaniya, **2**, 54 (2021). (in Russian) DOI: 10.31857/S1028096020110126
[21] A.K. Pikaev. Sovremennaya radiatsionnaya chimiya. *Tverdoe telo i polimery. Prikladnye aspekty* (Nauka, M., 1987), 448 s. (in Russian)
[22] S.V. Tsybulya, D.A. Yatsenko. Zhurnal strukturnoi chimii, **53**, 155 (2012). (in Russian)
[23] A.K. Shtol'ts, A.I. Medvedev, L.V. Kurbatov. *Rentgenovskii analiz mikronapryazhenii i razmera oblastei kogerentnogo rasstoyaniya v polikristallicheskikh materialakh* (UGTU-UPI, Ekaterinburg, 2005), s. 2–23. (in Russian)
[24] F.R. Studenikin. *Modifikatsiya puchka uskorennykh elektronov dlya povysheniya ravnomernosti radiatsionnoi obrabotki obluchaemykh obektov* (Kand. diss., MGU., M., 2022), s. 41–45. (in Russian)
[25] Z. Joi. Polimer J., **22**, 909 (1990).
[26] V.I. Poddubnyi, V.K. Lavrent'ev. *O forme amorfnogo galo na difraktogramme amorfno-kristallicheskikh polimerov* (Institut vysokomolekulyarnykh soedinenii, M., 1989), p. 354–356. (in Russian)
[27] S.S. Dong, W.Z. Shao, L. Vang, H.J. Ve, L. Zhen. RSC Adv., **8**, 28152 (2018). DOI: 10.1039/C8RA05744C
[28] L.A. Oksent'evich, M.M. Badaeva, G.I. Tuleninova, A.N. Pravednikov. Vysokomolek. soed., **19** (3), 553 (1977). (in Russian)
[29] P.H. Hermans, J.W. Street. Makromolek. Chem., **74** (1), 133 (1964).
[30] N.L. Mathakari, V.N. Bhozaskar, D.D. Sanjay. Mater. Sci. Eng.: B. **168** (1–3), 122 (2010). https://doi.org/10.1016/j.mseb.2009.11.005
[31] F. Uoker. *Khimicheskie i fizicheskite svoistva ugleroda* (Mir, M., 1969), p. 366. [Per. s angl.: P.L. Walker. *Chemistry & Physics of Carbon* (Marcel Dekker, NY., 1969), v. 4.]
[32] E.A. Plis, D.P. Engelhart, R. Cooper, W.R. Johnston, D. Ferguson, R. Hoffmann. Adv. Polyimide Films: Preparation, Properties and Applications, **9** (10), 1999 (2019). https://doi.org/10.3390/app9101999

Translated by M.Shevelev